nature portfolio

Peer Review File

Generation of out-of-plane polarized spin current by non-uniform oxygen octahedral tilt/rotation

Editorial Note: Parts of this Peer Review File have been redacted as indicated to remove third-party material where no permission to publish could be obtained.

REVIEWER COMMENTS

Reviewer #1 (Remarks to the Author):

The submitted manuscript, “Generation of out-of-plane polarized spin current by non-uniform oxygen octahedral tilt/rotation” is a very clear and thorough paper in which the authors are able to tune the structure of a metallic oxide, CaRuO3, in order to allow transmission of a spin current polarized out-of-plane – a configuration generally forbidden by crystalline symmetry. Materials with perpendicular magnetic anisotropy (PMA) have become favorable for spintronic devices due to their ability to scale to smaller lateral sizes. Using techniques well-established in the field, the authors demonstrate both 1. that spin current of this configuration can be transmitted, and 2. that it can be used to switch the magnetization direction of a prototypical ferromagnet device with PMA. While there have been many studies on the effects of crystalline symmetry on the material properties of complex oxides, this work represents a very nice application of these principles to the field of spin-orbit torques.

The methodology is thorough, with a significant amount of supporting measurements included in the supplementary information. The authors explain very clearly for a broader audience the significance of the different symmetries, numerical methodologies, and the significance of the different torque components (field-like, damping-like, and in different orientations) extracted from the measurements. They also clearly explain the modelling and fitting so that others can reproduce the work.

I have a few minor suggestions and questions:

1. The authors have a very nice discussion and diagrams of the crystalline symmetries which are broken by the relaxation of the octahedral rotation pattern. However, besides orthorhombic materials, many cubic or tetragonal materials undergo strain relaxation causing a change in the crystalline symmetry through the film (e.g. change in lattice parameters). Would this type of broken symmetry still forbid a perpendicular spin current polarization, or would the current be too small in comparison to the other components? Can the authors comment on why this type of broken symmetry would not yield similar results?

2. When discussing the MOKE results in the text, the authors say that the pillar “turns white” before discussing the magnetization switching, which is confusing because the physical color of the material does not change with magnetization, and the actual colors used to plot the MOKE polarization is arbitrary.

3. The authors mention that the CaRuO3 film becomes twinned as it relaxes, since the cubic structure of the substrate cannot prefer a direction for a vs. b. Is there any evidence for this in the STEM data? This results in isotropic behavior between the 110 and 1-10 axes in ST-FMR measurements, but is this also confirmed for the original resistivity measurements? What axis is the current direction for supplemental figure S5?

4. For the more general audience of Nature Communications who is unfamiliar with FMR measurements, I would suggest adding the magnetization/precession to the schematic in Fig

3a.

Reviewer #2 (Remarks to the Author):

The authors have investigated the generation of spin currents in a symmetric quasi-perovskite CRO. This would be a novel attempt that has potential for application to devices, etc., depending on the development of future research. But I don't recommend this paper for the following reasons: I. suspicion of Joule heating generation due to the sample quality, II. possibility of ferromagnetism, III. few references on CRO properties.

I. Suspicion on Joule heating generation
The authors grown the CRO films under the low oxidation condition. It is thought to measure the electron diffusion due to Joule heat generated in the low-quality samples.
The defects in CRO film
The oxygen condition of 30 Pa in this study is insufficient even for smaller 1.5 J/cm2 fluence [Daptary et al. (2017). Physica B: Condensed Matter, 511, 74-79.]. The large roughness and defects on surface were reported by AFM/SEM. Indeed, the upturn of resistivity at low temperature in this study is same as the reported behavior of CRO film grown under low oxidation condition. The electrical resistivity of the samples in this study is even higher. It has been reported that the difference in oxidation conditions causes differences in conduction.
The crystallinity of CRO film
As mentioned by the author as 'broad peak (line 110)', the FWHM of ~ 0.5 deg. is large as shown in out-of-plane XRD [Nair et al. (2018). APL Materials, 6(4).]. I don’t agree with ‘high crystalline quality (line 113)’. The broad XRD peak shows the disorder of the crystal and the possibility of impurities.
The low crystal quality causes to amounts of Joule heat, leading to misinterpretation on the measured voltage. High-grade samples with low electrical resistivity enable us to measure accurate voltage by high current to suppress Joule heat generation. The power of 15 dBm is so large for the small sample (Fig. 3). Pulse current of Jc = 7x1010 A/m2 is also large (Fig. 4). This is six orders of magnitude more than typical physical property measurements and is comparable to the gold breaking current. It is considered that electron diffusion due to Joule heating and its magnetic field effects appear.
Since CRO locates on the quantum critical region [Cao et al. (2008). Solid State Communications, 148(7-8), 305-309.], a little difference in growth conditions causes to a huge difference on conduction [Rao et al. (1997). Applied physics letters, 70(22), 3035-3037.]. It is noted that CRO compound can be accurately measured on high-quality and homogeneous samples.

II. Is CRO paramagnetic? (lines 23 and 67)
The (weak) ferro on CRO was reported in [Koriyama et al. (2004). Journal of alloys and compounds, 372(1-2), 58-64., Chen et al. (2010). Applied Physics Letters, 96(18)., Tripathi et al. (2014). Scientific reports, 4(1), 3877.]. I speculate that the properties in this report are originated from ferromagnetism.

III. Few references and their discussion of properties on CRO
The physical properties of CRO have been reported, but the authors do not discuss them.

・ The STEM-HAADF and ABF observations (Fig. 1)

‘the gradual change of octahedral tilt/rotation along the out-of-plane direction’ was reported

in [Sakoda et al. (2023). Advanced Electronic Materials, 2201312.]. This figure contains a small amount of new information, therefore is not sufficient worth to publish.

・ The band structure (Fig. 2)

The Fermi surface of CRO was clarified by ARPES [Liu et al. (2018). Physical Review B, 98(4), 041110.] and SdH effect [Schneider et al. (2014). Physical Review Letters, 112(20), 206403.]. Focusing on the Fermi energy in Fig. 2d, the convincing reason is required to explain the difference against the experimental fact.

Minor comments
'Pane' in lines 21, and 49.
The references of 1 and 7 are same.
No crystal axes in Fig2b and FigS2b.

Reviewer #3 (Remarks to the Author):

In this manuscript, the authors demonstrate field-free switching of perpendicular magnetization via spin-orbit torque. The device consists of a CRO film with ferromagnetic CoFeB and exhibits a low switching current density. Overall, the experiments are systematically executed with a reasonable theory. The results of this manuscript are interesting and informative, but the paper requires more explanations as follows.

- Besides SOT efficiency, the numerical value of the spin Hall angle or effective magnetic field is a more tangible parameter to estimate the spin characteristic of this material. In addition, a comparison of these parameters with a similar system should be helpful for evaluating this channel.
- In Fig. 4b, isn't Hex related to the switching current?
- In Fig. 4c and d, the grey colors correspond to +Mz and –Mz, respectively. I am wondering why the grey color does not represent the same direction. Additionally, for example, in Fig. 4c, I intuitively assume that the grey color may correspond to the in-plane direction of magnetization. If the magnetization is along the in-plane direction, which color is presented in the image?
- The curves are shifted for visualization in Fig. 4b. Including information about the baseline resistance in the caption would be helpful for readers.
- In the switching experiment shown in Fig. 4, the current is divided into two paths: the CRO channel and metallic multilayers. The portion of the current for each of the two paths should be clarified in the manuscript.
- On page 6, the authors explain that 'The influence of the Py/CRO interface is very limited...' This sentence may mislead readers because the authors describe an out-of-plane polarized spin current resulting from the relaxation of oxygen octahedral tilt/rotation near the interface.
- The experiment on the switching of perpendicular magnetization involves x- and y-direction polarized current, as well as z-direction polarized current. What are the relative values of these three terms?
- The authors claimed that a very low current density is required for switching. A comparison with other field-free systems is recommended.
- Please discuss the dot size effect and pulse width effect on critical switching current density.
- Please describe the role of Ti between CRO and CoFeB.

(Minor comments)
- In Fig. 3a, the arrowhead of the spin current (J_S) may be obscured by other objects.
- In Fig. 4a, inserting the direction of Hex is helpful for readers to easily understand the experimental set-up.
- In addition to current density, information about the actual current itself in Fig. 4b may be helpful for future experiments conducted by others.
- The insertion of a scale bar or a description of dot size in the caption of Fig. 4c and d is recommended.

I will recommend this manuscript for publication if these issues are clearly addressed.

Response Letter

Reply to Reviewer #1

General Comment: *"The submitted manuscript, "Generation of out-of-plane polarized spin current by non-uniform oxygen octahedral tilt/rotation" is a very clear and thorough paper in which the authors are able to tune the structure of a metallic oxide, $CaRuO_3$, in order to allow transmission of a spin current polarized out-of-plane – a configuration generally forbidden by crystalline symmetry. Materials with perpendicular magnetic anisotropy (PMA) have become favorable for spintronic devices due to their ability to scale to smaller lateral sizes. Using techniques well-established in the field, the authors demonstrate both 1. that spin current of this configuration can be transmitted, and 2. that it can be used to switch the magnetization direction of a prototypical ferromagnet device with PMA. While there have been many studies on the effects of crystalline symmetry on the material properties of complex oxides, this work represents a very nice application of these principles to the field of spin-orbit torques.*

The methodology is thorough, with a significant amount of supporting measurements included in the supplementary information. The authors explain very clearly for a broader audience the significance of the different symmetries, numerical methodologies, and the significance of the different torque components (field-like, damping-like, and in different orientations) extracted from the measurements. They also clearly explain the modelling and fitting so that others can reproduce the work."

Reply: We thank the reviewer for the high evaluation of our work and pointing out the novelty and significance of our results.

Comment 1: *"The authors have a very nice discussion and diagrams of the crystalline symmetries which are broken by the relaxation of the octahedral rotation pattern. However, besides orthorhombic materials, many cubic or tetragonal materials undergo strain relaxation causing a change in the crystalline symmetry through the film (e.g. change in lattice parameters). Would this type of broken symmetry still forbid a perpendicular spin current polarization, or would the current be too small in comparison to the other components? Can the authors comment on why this type of broken symmetry would not yield similar results?"*

Reply: We thank the reviewer for the high evaluation of our symmetry analysis and the valuable comment. We agree with the reviewer that the strain relaxation can change crystal symmetry generally. The perpendicular spin current polarization will be forbidden due to some symmetry constrains, and the CRO system in this work is one of the best material candidates. Following the reviewer's suggestion, we have performed a complete symmetry analysis.

First, we give a general symmetry analysis. The z-polarized spin current is forbidden by C_{nc}, $\widetilde{C_{nc}}$, M_c, $\widetilde{M_c}$, and the coexistence of in-plane symmetries M_a and M_b (M_a can be substituted by $\widetilde{M_a}, C_{2a}$ *or* $\widetilde{C_{2a}}$; M_b can be substituted by $\widetilde{M_b}, C_{2b}$ *or* $\widetilde{C_{2b}}$), and some other crystalline symmetries. Here "~" denotes the nonsymmorphic symmetries. Generally, the strain relaxation or change in lattice parameters could hardly break the symmetries C_{2c}, M_a, M_b and the nonsymmorphic symmetries without z-direction translation in bulk and films stacked along z-axis. The nonsymmorphic symmetries involving z-direction translation can be broken by the

nonuniformity of the strain or the change in lattice parameters along z-axis.

However, space groups which can yield such results of forbidden perpendicular spin current polarization, are quite limited. We have investigated the 3D space symmetry groups from No. 75 to No. 142 for tetragonal materials and from No. 195 to No. 230 for cubic materials. We found that only ($P4_1$, $P4_3$, $P4_122$, $P4_12_12$, $P4_322$, $P4_32_12$, $P2_13$, $Pa\bar{3}$, $P4_132$, $P4_332$, $Fd\bar{3}m$, $Fd\bar{3}c$) 12 groups have nonsymmorphic symmetries with z-direction translation and satisfy other symmetry constraints among the 104 space groups. Tetragonal or cubic materials with these symmetry groups can be a potential source of z-direction polarized spin Hall current from symmetry breaking near the interface.

Second, we confirm on the concrete materials discussion. In bulk CRO, the perpendicular spin current polarization is forbidden by nonsymmorphic symmetries $\widetilde{C_{2b}}$, $\widetilde{C_{2c}}$, $\widetilde{M_b}$ and $\widetilde{M_c}$ involving a half-lattice translation along c (i.e. z) direction, which would be obviously broken due to the nonuniform rotation and tilt of oxygen octahedra in the CRO films near the interfaces. The restore of these symmetries takes at least 18 unit cells from our experiments. It reveals that the materials with nonsymmorphic symmetries translated along z direction and none of other forbidding symmetries will be free of the symmetry constraints on the z-polarized spin Hall current under the strain relaxation or change in lattice parameters. Therefore, the CRO structure is a good system to generate perpendicular spin current polarization in thin films and heterostructures.

Usually, gradual strain relaxation occurs when the thickness of the films reaches several tens of nanometers, and amplitude of lattice constant changes caused by strain relaxation is relatively limited. So, it's hard to ensure the generation of obvious z-direction polarized spin current. Compared to the tetragonal or cubic materials, CRO has large oxygen-octahedral rotation/tilt angle. In the absence of strain relaxation, the obvious relaxation of oxygen octahedral occurs due to the coupling with substrate, which significantly regulates the Ru-O bond hybridization [Lee, J. *et al.* Appl. Phys. Lett. 117, 163906 (2020)]. Besides the satisfactory of symmetry constraints, large spin Hall effect requires that the material should have strong spin-orbit coupling effect and adequate density of states near the Fermi surface, which is shown in CRO from our DFT calculations. The above reasons enhance the perpendicular spin current polarization in CRO.

Following the valuable comment, we add more explanation on this point in the revised manuscript (Page 8, Line 298-309).

Comment 2: *"When discussing the MOKE results in the text, the authors say that the pillar "turns white" before discussing the magnetization switching, which is confusing because the physical color of the material does not change with magnetization, and the actual colors used to plot the MOKE polarization is arbitrary."*

Reply: We thank the reviewer for pointing out the question. This measurement is based on background-subtracted MOKE. To enhance the contrast, the background in the whole image was subtracted, thus, the whole image in the initial state maintains the same color (grey) though the pillar area is in magnetic polarity state. In Figs. 4c and 4d, we initialize the magnetization to the $+M_z$ state and $-M_z$ state, respectively, and the images of the initial state are both grey after the background is

subtracted. When the magnetic polarity state changes, the color in pillar area changes accordingly, while the color outside the pillar area remains unchanged. Although the grey color does not represent the same magnetic polarity state, the $-M_z$ state is always brighter than the $+M_z$ state. This MOKE measurement method is widely used to characterize magnetic polarity state, for example the study in Liu, L. *et al.* Nat. Nanotechnol. 16, 277-282 (2021) and Davies, C.S. *et al.* Nature, 628, 540–544 (2024).

Here, we further clarify the process of magnetization switching by MOKE measurement. The switching of magnetization has been confirmed by background-subtracted MOKE measurement in the manuscript. Fig. 4c shows the background-subtracted MOKE images of field-free SOT switching magnetization from $+M_z$ state to $-M_z$ state. We initialize the magnetization of the pillar structure to $+M_z$ state by applying a saturation magnetic field along the $+z$ direction and the initial contrast of image is grey after the background is subtracted. Then the external field is set back to zero, when a –10 mA pulsed current is applied into the channel, the pillar area turns white totally, indicating that the magnetization has changed from the $+M_z$ state to the $-M_z$ state totally. After the application of the +10 mA electric pulse, the pillar area turns back to grey, i.e. the magnetization turns back to the $+M_z$ state. In order to confirm the process of magnetization switching, we initialize the magnetic moment to the $-M_z$ state and the contrast is gray after the background is subtracted, as shown in Fig. 4d. The device takes the $+M_z$ state after the electric pulse of +10 mA, then turns back to the $-M_z$ state after the –10 mA electric pulse.

Considering the comments of the reviewer, we add the relative caption of MOKE measurement to help the audience to easily understand (Page 17, Line 576-578), and update the description of experimental results in the revised manuscript (Page 9, Line 341-353).

Comment 3: *"The authors mention that the $CaRuO_3$ film becomes twinned as it relaxes, since the cubic structure of the substrate cannot prefer a direction for a vs. b. Is there any evidence for this in the STEM data? This results in isotropic behavior between the [110] and [1$\bar{1}$0]-axes in ST-FMR measurements, but is this also confirmed for the original resistivity measurements? What axis is the current direction for supplemental figure S5?"*

Reply: We agree that the STEM is a typical method for studying the microstructure of thin films, and several kinds of twinned domain structure can be recognized with the help of selected area electron diffraction (SAED) measurements. However, this kind of twinned domain structure in this CRO films results in same electron diffraction pattern, so it's hard to be recognized, which has been confirmed in the study of CRO structure by SAED measurements [Jiang, J. C. *et al.* J. Appl. Phys. 89, 6365–6369 (2001); Jiang, J. C. *et al.* Appl. Phys. Lett. 72, 2963–2965 (1998)]. Thus, we measure the reciprocal space mappings (RSMs) for the (103) reflections of CRO films at different phi angles as shown in Fig. R1a. The (103) reflections of CRO films show a fourfold symmetry implying the twinned crystal domains, different from the twofold symmetry of orthogonal structure.

We further study the anisotropy between the [110] and [1$\bar{1}$0]-axes by resistivity measurements. The CRO (9 nm) films grown on LAO substrate were etched into devices which are along [110] and [1$\bar{1}$0]-axes, respectively, as shown in Fig. R1b. The measurement results indicate that the resistivity along the [110] and [1$\bar{1}$0]-axes exhibits the same behavior and the upturn is at the same temperature

as shown in Fig. R1c. The difference of resistivity between the two axes is pretty small. The resistivity measurements further confirm the isotropic behavior between the [110] and [1$\bar{1}$0]-axes. The current direction is along one of [110] and [1$\bar{1}$0]-axes in fig. S7 of Supplemental Information.

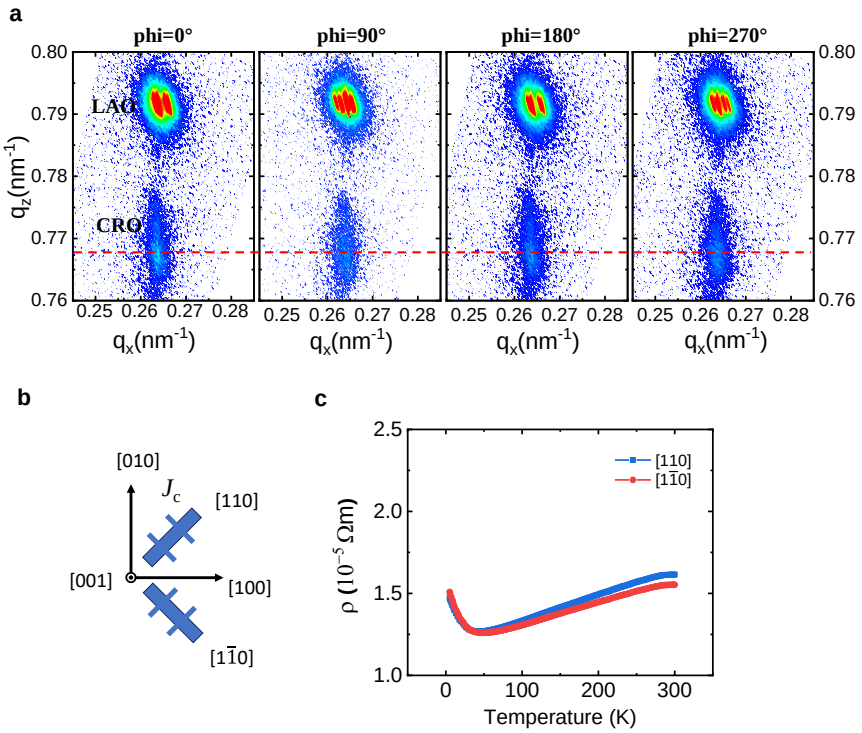

Fig. R1 a, Reciprocal space mappings (RSMs) for the (103) reflections of CRO film grown on LAO substrate at different phi. The red dashed line marks the peak of CRO film. b, Schematic setup of devices along [110] and [1$\bar{1}$0]-axes, respectively. c, Four-terminal resistance as a function of temperature for CRO films along [110] and [1$\bar{1}$0]-axes, respectively.

The discussion of anisotropy resistivity measurements is added in the revised manuscript (Page 3, Line 123-126) and the figures is added in Section 3 of Supplementary Information.

Comment 4: *"For the more general audience of Nature Communications who is unfamiliar with FMR measurements, I would suggest adding the magnetization/precession to the schematic in Fig 3a."*

Reply: We thank the reviewer for the valuable suggestion. We update the schematic of ST-FMR measurement in Fig. 3a in the revised manuscript, in which the magnetization and its precession driven by damping-like torque are added as shown in Fig. R2.

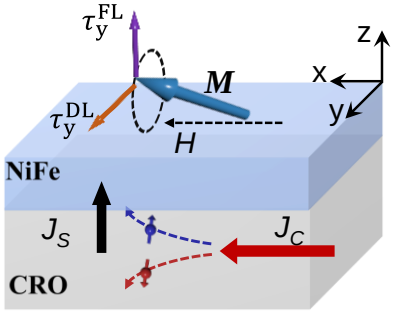

Fig. R2 Schematic of ST-FMR measurement with magnetization and precession.

Reply to Reviewer #2

General Comment: *"The authors have investigated the generation of spin currents in a symmetric quasi-perovskite CRO. This would be a novel attempt that has potential for application to devices, etc., depending on the development of future research. But I don't recommend this paper for the following reasons: I. suspicion of Joule heating generation due to the sample quality, II. possibility of ferromagnetism, III. few references on CRO properties."*

Reply: We thank the reviewer for acknowledging that "*This would be a novel attempt that has potential for application to devices, etc., depending on the development of future research*". For the concern on the three points, we perform additional experiments to further confirm our results and declare these questions. We wish that the reviewer can now be convinced and support the publication of our work in Nature Communications.

Comment 1: *"I. Suspicion on Joule heating generation*
The authors grown the CRO films under the low oxidation condition. It is thought to measure the electron diffusion due to Joule heat generated in the low-quality samples.

The defects in CRO film
The oxygen condition of 30 Pa in this study is insufficient even for smaller 1.5 J/cm2 fluence [Daptary et al. (2017). Physica B: Condensed Matter, 511, 74-79.]. The large roughness and defects on surface were reported by AFM/SEM. Indeed, the upturn of resistivity at low temperature in this study is same as the reported behavior of CRO film grown under low oxidation condition. The electrical resistivity of the samples in this study is even higher. It has been reported that the difference in oxidation conditions causes differences in conduction.

The crystallinity of CRO film
As mentioned by the author as 'broad peak (line 110)', the FWHM of ~ 0.5 deg. is large as shown in out-of-plane XRD [Nair et al. (2018). APL Materials, 6(4).]. I don't agree with 'high crystalline quality (line 113)'. The broad XRD peak shows the disorder of the crystal and the possibility of impurities.

The low crystal quality causes to amounts of Joule heat, leading to misinterpretation on the measured voltage. High-grade samples with low electrical resistivity enable us to measure accurate voltage by high current to suppress Joule heat generation. The power of 15 dBm is so large for the small sample (Fig. 3). Pulse current of $Jc = 7x10^{10}$ *A/m*^{2} *is also large (Fig. 4). This is six orders of magnitude more than typical physical property measurements and is comparable to the gold breaking current. It is considered that electron diffusion due to Joule heating and its magnetic field effects appear.*

Since CRO locates on the quantum critical region [Cao et al. (2008). Solid State Communications, 148(7-8), 305-309.], a little difference in growth conditions causes to a huge difference on conduction [Rao et al. (1997). Applied physics letters, 70(22), 3035-3037.]. It is noted that CRO compound can be accurately measured on high-quality and homogeneous samples."

Reply: We agree that spin current can just be accurately measured on high-quality and homogeneous samples, thus, the crystal quality is further characterized. In addition, the contribution of Joule heating in ST-FMR measurements as well as the temperature rise due to Joule heating in SOT switching are analyzed.

Crystal quality of CRO films

The environment of the cavity varies among different pulsed laser deposition, so it is necessary to directly characterize the quality of the CRO films. In order to reduce the defects, the CRO films are cooled to room temperature in an oxygen pressure of 100 Pa after deposition. From the atomic force microscope (AFM) image of CRO films shown in Fig. R3a, we can see that CRO films have good quality. **The RMS (root mean square) surface roughness extracted from the image is about 0.4 nm,** indicating that CRO films in this study have lower surface roughness compared to the referenced results (0.8 nm) of CRO films grown under high oxidation condition [Daptary. G. N. *et al.* Physica B Condens. Matter 511, 74-79, (2017)].

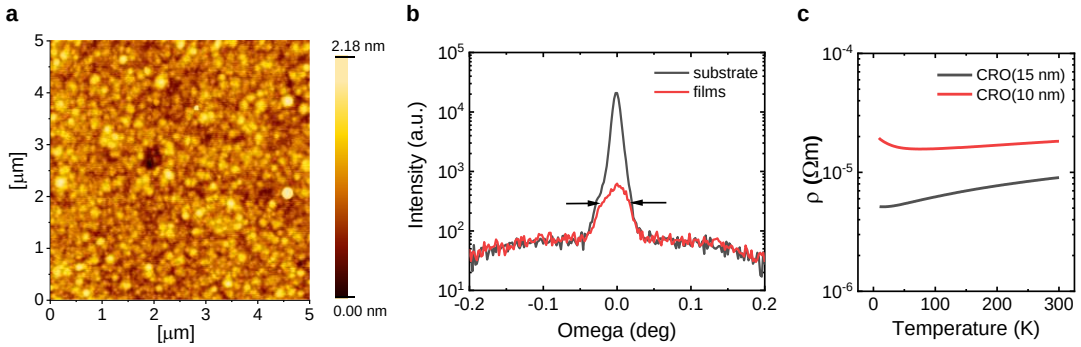

Fig. R3 a, Atomic force microscope (AFM) image of CRO films, b, Rocking curve of CRO (10 nm) films grown on LAO substrate. c, Resistivity of the CRO films with different thickness as a function of temperature.

The peak of CRO films in XRD spectrum broadens under the strain from substrate, and the full width at half maximum (FWHM) is about 0.5 deg which is comparable to the referenced results (0.4 deg) of CRO films [Nair, H. P. *et al.* APL Mater. 6, 046101 (2018)]. The XRD spectrum of CRO films usually possesses a broadening about 0.5 deg, which can ensure the crystallinity [Daptary. G. N. *et al.* Physica B Condens. Matter 511, 74-79, (2017)]. Further, the rocking curve is measured to characterize the quality of CRO (10 nm) films as shown in Fig. R3b, **and the FWHM is about 0.03 deg which is also comparable to the referenced results (0.02 deg) of CRO films** [Nair, H. P. *et al.* APL Mater. 6, 046101 (2018)]. Furthermore, the broadening of the rocking curve is within that of substrate, indicating a good crystallinity. The low intensity and broadening of curves are due to the smaller thickness of the films (10 nm) compared to the referenced results (32 nm). The AFM image and XRD spectrum confirm that CRO films is fabricated under proper conditions.

Generally, the resistivity of the CRO films is closely related to the thickness, the CRO films with thickness of 10 nm shows a small upturn in resistivity, while, the resistivity persists metallic behavior when the thickness increases to 15 nm as shown in Fig. R3c. Thus, the upturn behavior cannot be attributed to the low oxidation condition. The dependence of resistance on thickness in Fig. R3c is consistent with the reported results [Ali, Z. *et al.* npj Quantum Mater. 7, 108 (2022)].

Therefore, the CRO films is homogeneous and have good crystallinity.

The analysis of crystal quality is added in Section 1 of Supplementary Information, and the corresponding discussion is added in the revised manuscript (Page 3, Line 115-117).

Contribution of Joule heating effect in SOT efficiency

We thank the reviewer for insightful advice about whether the microwave power of 15 dBm is large for Joule heating effect in ST-FMR devices. As mentioned in Kondou, K. *et al.* Nat. Phys. 12, 1027–1031 (2016), **the linear relationship between the appropriate power and symmetric component of ST-FMR signal can ensure the correctness of the shape of the ST-FMR curves, thus eliminating the influence of thermal effect induced by microwave power.** To further exclude Joule heating effect from microwave power, we have measured the microwave-power-dependent ST-FMR signal in the CRO/Py device at 5 GHz from 9 to 19 dBm (as shown in Fig. R4a). As the power increases, the voltage of the symmetric component V_S in our device varies linearly with the power, which demonstrates the magnetization precession is in the linear regime (from 9 to 16 dBm). And deviate from linearity at higher power (from 17 to 19 dBm), which implies Joule heating effect from higher microwave power. **The ST-FMR measurement for SOT efficiency is under the power of 15 dBm without obvious Joule heating effect, thus the SOT efficiency can be accurately determined.**

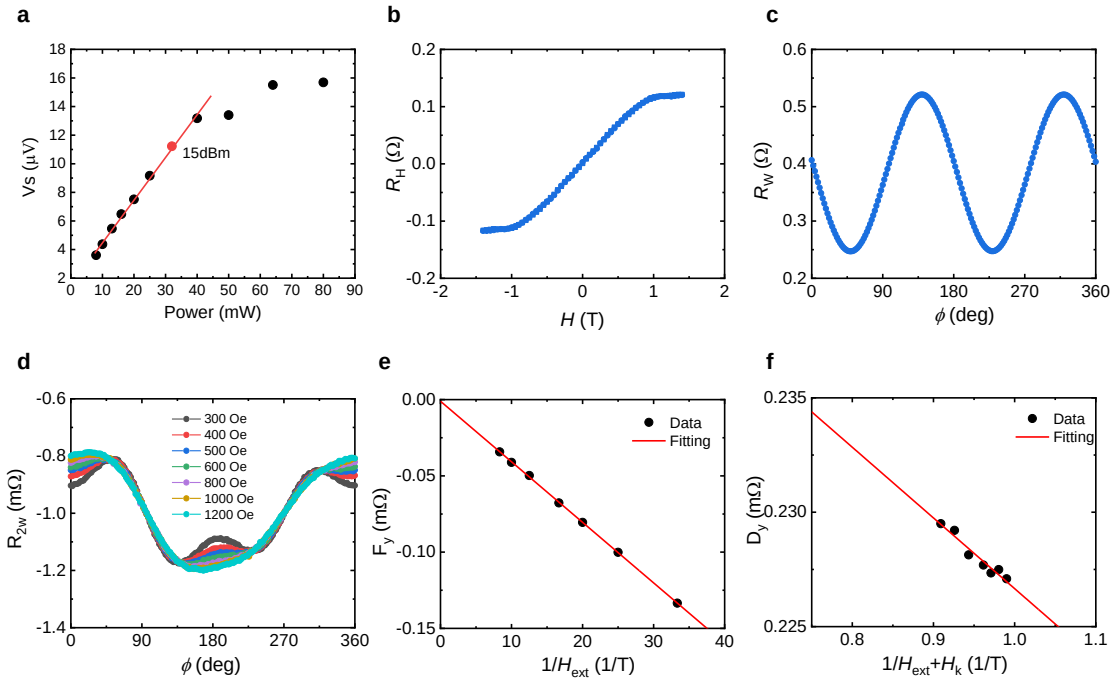

Fig. R4 a, Microwave power dependence of V_S extracted from the ST-FMR signals. b, Perpendicular magnetic field dependence of the Hall resistance (R_H). c, First harmonic Hall resistance (R_ω) as a function of in-plane rotation angle ϕ. d, Second harmonic Hall resistance ($R_{2\omega}$) as a function of in-plane rotation angle ϕ, under different external magnetic field. e-f, Linear plot of F_y against $1/H_{ext}$ (e) and D_y against $1/H_{ext}+H_k$ (f).

In order to further distinguish the influence of the Joule heating on SOT efficiency measurement, we perform the second harmonic measurements which can separate the voltages from spin Hall effect and Joule heating effect. Actually, the Joule heating can cause spin current between the layers,

inducing additional resonant voltage signals, which exhibit a dependence on the angle of an in-plane magnetic field in the ST-FMR measurement that is identical to the signal from the SOT. The Py/CRO heterostructure is patterned into Hall bars with a width of 20 um. An ac current with frequency of 1.33 KHz is injected into the Hall bar, the current densities in CRO films is 2.57×10^5A/cm^2. The first (R_w) and second (R_{2w}) harmonic Hall voltages are measured using lock-in as a function of the external magnetic field angle as show in Figs. R4c and R4d, respectively. The SOT torque can be separated from the ϕ dependence voltage signals using following equation:

$$R_{2w} = F_y(2cos^3\phi - cos\phi) + D_y cos\phi + R_{ther} sin2\phi \quad (1)$$

with

$$F_y = 2R_{PHE}\frac{H_y^{FL}+H_O}{H_{ext}} \quad (2)$$

$$D_y = R_{AHE}\frac{H_y^{DL}}{H_{ext}-H_K} + R_{ANE} \quad (3)$$

Where D_y term consists of the contributions from both the damping-like torque coefficients generated by the spin Hall effect and the anomalous Nernst effect (R_{ANE}); F_y term is the superposition of field-like torque and Oersted field counterparts (y represents the direction of polarization). The R_{ther} term has been removed during data processing, which is likely to arise from a thermal gradient along the direction of current. The H_y^{DL} is y-polarized damping-like torque effective fields. The H_y^{FL} and H_O are y-polarized field-like torque effective fields and Oersted field, respectively. R_{AHE} is the coefficient of the peak anomalous Hall voltage as shown in Fig. R4b. R_{PHE} is the coefficient of the peak planar Hall effect voltage for the given amplitude of alternating current as shown in Fig. R4c. H_{ext} is external magnetic field and H_K characterizes the magnetic anisotropy. The $H_y^{FL} + H_O$ derived from linear fitting is 0.145 Oe indicating that field-like torque effective fields are pretty small as shown in Fig. R4e. The D_y against $\frac{1}{H_{ext}-H_K}$ is plotted to extract the H_y^{DL} from the gradient of the linear fit as shown in Fig. R4f. The good linear relation for the D_y against $\frac{1}{H_{ext}-H_K}$ is the direct evidence of a sizable damping-like torque. The torque efficiencies per unit electric field associated are:

$$\xi_{y,z}^{DL} = \frac{2eH_{y,z}^{DL}m_s}{\hbar J} \quad (4)$$

where J is the current density in the CRO layer, m_s is the saturation magnetization of the Py layer. **We find ξ_y^{DL}=1.2 at room temperature which is close to the efficiency from ST-FMR measurements (1.4). Thus, the SOT from spin Hall effect is dominant and Joule heating only contributes a small portion.**

The analysis of Joule heating effect in SOT efficiency is added in Section 9 of Supplementary Information, and the corresponding discussion is added in the revised manuscript (Page 6, Line 231-238).

Joule heating effect analysis for SOT switching measurement

As considered by the reviewer, a temperature rise is likely to be generated due to the Joule heating effect when the current flows through the Hall bar. Therefore, it is necessary to calibrate the instant device temperature at the switching point. We measure the resistance of device as a function of

temperature, for which a tiny dc current 10 μA is applied to avoid heating effect. As shown in Fig. R5a, a linear dependence is obtained. Then, we measure the exact resistance when applying pulsed current as shown in Fig. R5b. The pulsed current with density of 6.3×10^{10}Am^{-2} gives a resistance of 1150 Ω, and the instant device temperature is determined to be 354 K.

We further analyze the impact of temperature rise on the PMA layer. The anomalous Hall resistance curves versus out-of-plane magnetic field under different temperature are measured as shown in Fig. R5c. The CoFeB ferromagnetic layer is below the Curie temperature and maintains perpendicularly ferromagnetic when the temperature is 350 K. In addition, the coercive field decreases when the temperature rises, which result in the decrease of magnetic anisotropic energy. Thus, the critical current density will be slightly reduced with the assistance of Joule heating [Zhu, L. Adv. Mater. 35, 2300853 (2023)]. **However, the switching of perpendicular magnetization cannot be achieved solely by Joule heating, and the in-plane effective field from *z*-polarized spin current from CRO films is necessary for field-free switching of perpendicular magnetization.**

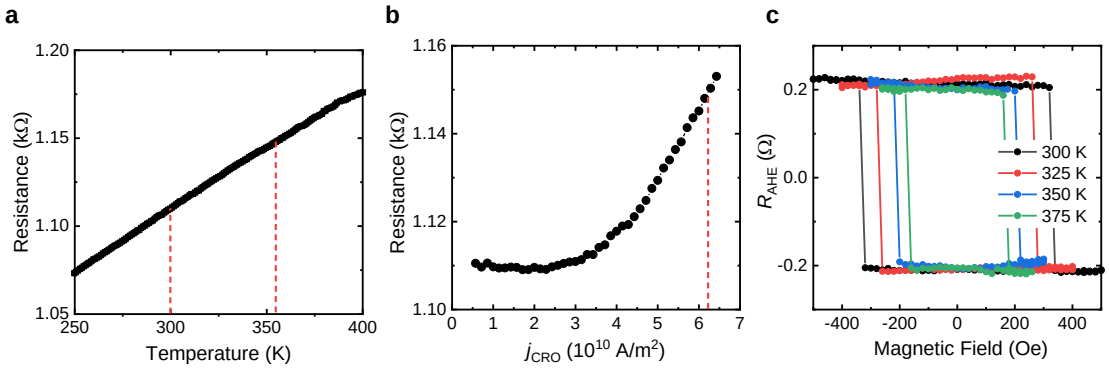

Fig. R5 a, Resistance of device as a function of temperature. b, Resistance of device as a function of the pulsed current density. c, Anomalous Hall resistance curves versus out-of-plane magnetic field under different temperature.

In summary, the CRO films are of high quality and homogeneous, and the SOT efficiency can be accurately determined. The Joule heating effect just leads to the increase of temperature and CoFeB still maintains perpendicularly ferromagnetic when the pulsed current is applied in CRO films. Thus, SOT plays a dominant role in the switching of magnetic moments, and switching cannot be achieved solely by Joule heating.

Considering the necessity of Joule heating effect analysis in spin current research, we add the related study of temperature rise at the switching point in Section 18 of Supplementary Information, the corresponding discussion is added in the revised manuscript (Page 9, Line 336-339).

Comment 2: *"Is CRO paramagnetic? (lines 23 and 67)*
The (weak) ferro on CRO was reported in [Koriyama et al. (2004). Journal of alloys and compounds, 372(1-2), 58-64., Chen et al. (2010). Applied Physics Letters, 96(18)., Tripathi et al. (2014). Scientific reports, 4(1), 3877.]. I speculate that the properties in this report are originated from ferromagnetism."

Reply: As considered by the reviewer, ferromagnetism does indeed lead to spin currents with out-of-plane polarization, we further analyze the magnetism of CRO films by Squid-VSM

measurements.

Zero-field-cooled (ZFC) and field-cooled (FC) magnetization curves taken after cooling the sample without applying a magnetic field and while cooling the sample in an applied magnetic field with 1000 Oe were measured, respectively. The curves of magnetization versus temperature (*M-T*) coincide very well for the FC and ZFC measurements down to 10 K as shown in Fig. R6a. The increase of magnetic moment with the decrease of temperature comes from the LAO substrate.

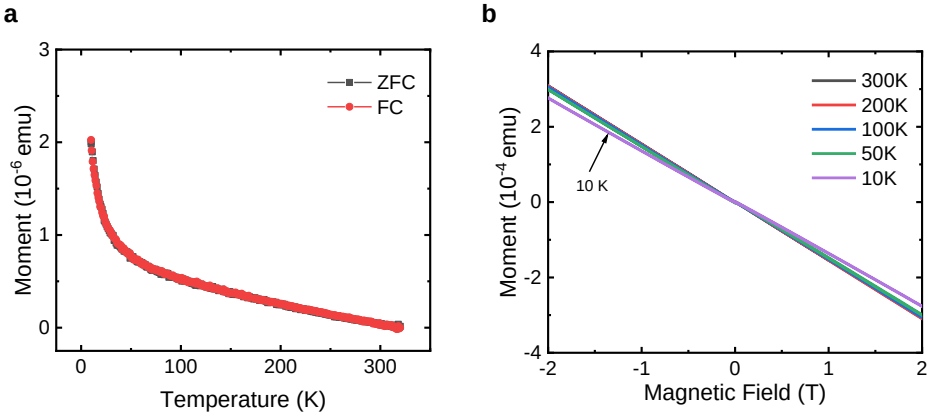

Fig. R6 a, Zero-field-cooled (ZFC) and field-cooled (FC) magnetization versus temperature plots for CRO (10 nm) films grown on LAO substrate. b, Magnetic-field dependence of magnetization for CRO films measured at different temperatures.

The curves of magnetization versus field (*M-H*) show almost linear field dependence from 50 K to 300 K as shown in Fig. R6b, suggesting that CRO films are paramagnetic. At 10 K, the *M-H* curve shows a slightly curvature under lower magnetic fields, indicating the existence of possible magnetic at low temperatures. Our measurement results are consistent with the published results referenced by reviewer that CRO films exhibit ferromagnetism at low temperatures. Due to the fact that both ST-FMR and switching measurements are performed at room temperature, it can be excluded that out-of-plane polarized spin currents originate from ferromagnetism.

The magnetization measurements are added in Section 11 of Supplementary Information and corresponding discussion is added in the revised manuscript (Page 6, Line 243-252).

Comment 3: *"Few references and their discussion of properties on CRO*

The physical properties of CRO have been reported, but the authors do not discuss them.

- *The STEM-HAADF and ABF observations (Fig. 1)*

'the gradual change of octahedral tilt/rotation along the out-of-plane direction' was reported in [Sakoda et al. (2023). Advanced Electronic Materials, 2201312.]. This figure contains a small amount of new information, therefore is not sufficient worth to publish."

Reply: We thank reviewer for this comment and providing this reference, but we have to emphasize that the engineering mechanism of the crystal structure and the corresponding change trend in octahedral tilt/rotation in our manuscript are exactly different from those of the reference. The comparison and discussion are presented in details as below.

1. **The gradual change of octahedral tilt/rotation can be attributed to the symmetry mismatch and coupling with substrate in our study, while it results from the tensile strain and growth conditions in the reference.** In the reference, the CRO films are grown on $NdGaO_3$ substrate which possesses orthorhombic structure and oxygen octahedral tilt/rotation same as bulk CRO materials. The growth conditions of Ca/Ru element ratio and the tensile strain from $NdGaO_3$ substrate regulate the structure of CRO films, further the relaxation of strain results in the gradual change of octahedral tilt/rotation. In our study, we constructed the symmetry-mismatched heterostructure by fabricating CRO films on LAO substrate which possesses cubic structure without octahedral tilt/rotation. Due to the mismatch and coupling with substrate, the octahedral tilt/rotation of CRO films is engineered near the interface. Based the comparison, we can conclude that the origins of gradual change in octahedral tilt/rotation are totally different.
2. **The corresponding trends of gradual change in octahedral tilt/rotation are opposite in these two cases.** In the reference, the CRO films show large tilt angle near the interface, and the tilt angle decreases when the CRO films are away from the interface as shown in Fig. R7a. However, in our study, the tilt angle is about zero when CRO films near substrate and increases when CRO films are away from substrate as shown in Fig. R7b. In addition, the gradual change of octahedral tilt/rotation in our manuscript sustains larger thickness. Therefore, the gradual change of octahedral tilt/rotation in CRO/LAO are different from that in CRO/$NdGaO_3$ heterostructure.

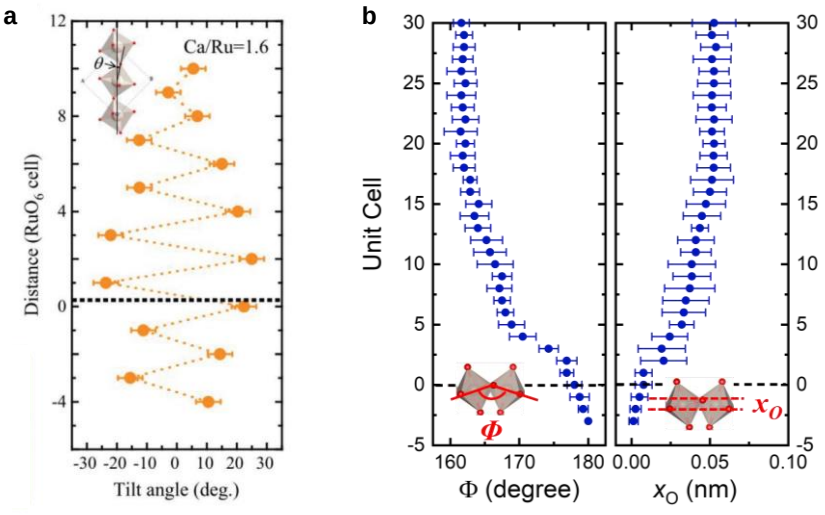

Fig. R7 a, Tilt angle as a function of the CRO layer in Figure 5f from this reference [Sakoda et al. (2023). Advanced Electronic Materials, 2201312.]. b, Averaged Ru-O-Ru bond angle Φ plotted as a function of the pseudo-cubic CRO layer from our manuscript.

Beyond the two points above from the perspective of structure, it is also noteworthy that we firstly investigate the out-of-plane spin current originated from the gradual change of octahedral tilt/rotation and realize field-free magnetization switching based on this spin current, which are not implemented in the reference.

In summary, in order to better display the gradual change of octahedral tilt/rotation and illustrate the mechanism of engineering crystal symmetry, we believe that the STEM-HAADF and ABF

observations in Fig. 1 provides new information and is necessary in our study. Meanwhile, we also agree that the reference provides the mechanism and corresponding results of regulating crystal structure, and we are sorry for not citing this reference. This reference and related discussion are added in the revised manuscript (Page 3, Line 108-113).

Comment 4: *"The band structure (Fig. 2)*
The Fermi surface of CRO was clarified by ARPES [Liu et al. (2018). Physical Review B, 98(4), 041110.] and SdH effect [Schneider et al. (2014). Physical Review Letters, 112(20), 206403.]. Focusing on the Fermi energy in Fig. 2d, the convincing reason is required to explain the difference against the experimental fact."

Reply: We thank the reviewer for these valuable suggestions.

Firstly, we discuss the Fermi surface. In Fig R8, we compare the Fermi surfaces from our calculations with the experimental ARPES spectra [Liu et al. Physical Review B, 98(4), 041110 (2018)] within the first BZ.

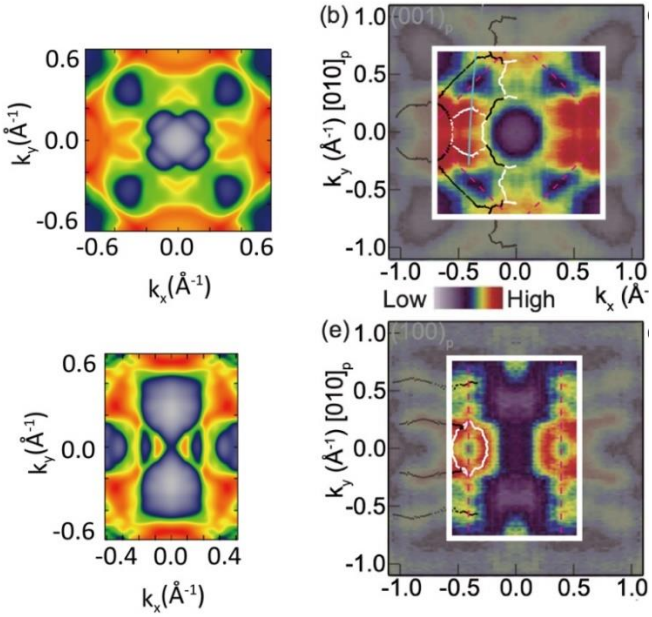

Fig. R8. (Left panels) Our simulated surface state spectrum at Fermi energy in first BZ. (Right panels) The experimental ARPES spectra from Fig 2(b) and (e) in Ref. [Liu, Y. *et al.* Phys. Rev. B, 98, 041110 (2018).]. The corresponding areas in the first BZ are marked with white boxes.

For both the (001) and the (100) surfaces, one can observe that our simulated surface states spectrum at the Fermi energy exhibit small pockets. And these small pockets locate at the similar positions as the experimental ones (see right panels of Fig. R8 in white box areas). Therefore, **our calculations are qualitatively consistent with the experimental results**.

Then we discuss the differences between our calculated band structures and the results shown in references [Liu, Y. *et al.* Phys. Rev. B, 98, 041110 (2018); Schneider, M. *et al.* Phys. Rev. Lett. 112, 206403 (2014).]. This is mainly due to three different calculating conditions:

1. Spin degree of freedom. In our calculations, we include the spin degree of freedom, as well as the spin-orbit coupling (SOC) effect, while the Schneider's work and the Liu's work treat the $CaRuO_3$ as a spinless system. Since we focus spin polarized Hall effect, the SOC effect should be considered.

2. Lattice parameters. In our calculations, we use the lattice parameters measured from our own samples, while the Schneider's work and the Liu's work all use the lattice parameters from reference [Zayak, A. T. *et al.* Phys. Rev. B 74, 094104 (2006)].
3. The type of the exchange-correlation functions in DFT. Our work and the Liu's work use the generalized gradient approximation (GGA), while the Schneider's work use the local-density approximation (LDA). In general, there is not much difference between the GGA and LDA methods, but GGA is more commonly used.

[Redacted]

Fig R9. (Left panel) Our calculated band structures without consideration of spin, using the LDA functionals. The lattice parameters are from [Zayak, A. T. *et al.* Phys. Rev. B 74, 094104(2006)]. (Right panel) The band structures from Fig 8. in the Supplemental material of [Schneider, M. *et al.* Phys. Rev. Lett. 112, 206403 (2014)].

According to their calculation conditions, we have well reproduced the band structures in the Schneider's work, as shown in Fig R9. The band structures in the Liu's work are not calculated on an experimental structure. But Liu claimed their results are in consistent with Ref. [Dang, H. T. *et al.* Phys. Rev. Lett. 115, 107003 (2015)], of which the calculations are performed on the experimental orthorhombic structure. We have well reproduced the band structures in the Dang's work, as shown in Fig R10.

[Redacted]

Fig R10. (Left panel) Our calculated spinless band structures by using the GGA functional. The lattice parameters are from [Zayak, A. T. *et al.* Phys. Rev. B 74, 094104 (2006)]. (Right panel) The band structures from Fig 2(c) of [Dang, H. T. *et al.* Phys. Rev. Lett. 115 107003 (2015)].

To sum up, our Fermi surface calculations are consistent with the experimental results. Our calculations are reliable and in good agreement with our experimental spin Hall results. The corresponding discussion of calculations results is added in the revised manuscript (Page 4, Line 160-165).

Minor comments

'Pane' in lines 21, and 49.

The references of 1 and 7 are same.

No crystal axes in Fig2b and FigS2b.

Reply: We thank the reviewer for pointing out these typos. The word "pane" is corrected to "plane" in lines 21, and 49 in the revised manuscript.

We delete the reference 7 and further check the references in the revised manuscript.

The crystal axes are added in Fig. 2b and Fig. S4b, and the related figure is updated in the revised manuscript.

Reply to Reviewer #3

General Comment: *"In this manuscript, the authors demonstrate field-free switching of perpendicular magnetization via spin-orbit torque. The device consists of a CRO film with ferromagnetic CoFeB and exhibits a low switching current density. Overall, the experiments are systematically executed with a reasonable theory. The results of this manuscript are interesting and informative, but the paper requires more explanations as follows. I will recommend this manuscript for publication if these issues are clearly addressed."*

Reply: We thank the reviewer for the high evaluation of our work and recommendation of publication of this manuscript in *Nature Communications*, the constructive suggestions from the reviewer will help us improve the quality of this manuscript.

Comment 1: *"Besides SOT efficiency, the numerical value of the spin Hall angle or effective magnetic field is a more tangible parameter to estimate the spin characteristic of this material. In addition, a comparison of these parameters with a similar system should be helpful for evaluating this channel."*

Reply: We agree that effective magnetic field is a tangible parameter to estimate the spin characteristic, thus the second harmonic measurement is performed as shown in Fig. R11. The damping-like torque effective magnetic field is proportional to the slope of the linear plot of D_y against $1/H_{ext}+H_k$ and estimated to be 10.5 Oe/(10^{10} Am^{-2}).

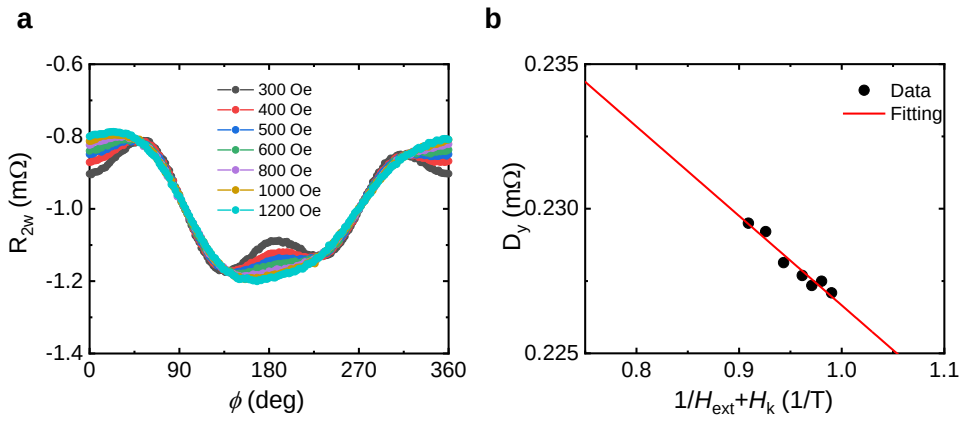

Fig. R11 a, Second harmonic Hall resistance ($R_{2\omega}$) as a function of in-plane rotation angle ϕ, under different external magnetic fields. b, Linear plot of D_y against $1/H_{ext}+H_k$.

According to the suggestion from the reviewer, we compare the parameters (i.e. effective magnetic field from second harmonic measurement and SOT efficiency from ST-FMR measurement) in a series of 4*d*/5*d* transition oxides (Table 1).

It can be found in Table 1 that, due to the strong spin-orbit coupling, 4*d*/5*d* transition oxides usually have a high efficiency for charge-spin interconversion. By comparing the effective magnetic field and SOT efficiency, we can see that the CRO films provide one of the largest efficiencies of charge-spin interconversion among 4*d*/5*d* transition oxides. In addition to high SOT efficiency, CRO films can also provide in-plane effective fields for field-free switching of perpendicular magnetization, making it a competitive material for high-performance magnetic memory and spin logic.

Table 1. Comparison of the effective magnetic field from second harmonic measurement and SOT efficiency from ST-FMR measurement of 4*d*/5*d* transition metal oxides from recent works.

Year	Author	Heterostructures	thickness	effective field ($/10^{10}$ Am^{-2})	SOT efficiency ($\hbar$/2e)	Temperature
this work	Han, F. *et al.*	$CaRuO_3$/Py	10 nm	10.5 Oe	1.4	300 K
2023[1]	Li, S. *et al.*	$SrRuO_3$/Py $SrRuO_3$/CoPt	20 nm	1.38 Oe (θ=0.18) 3.96 Oe (θ=0.21)	—	300 k
2023[2]	Li, P. *et al.*	$SrIrO_3$/CoFeB	10.8 nm	3.57 Oe	1.4	300 K
2019[3]	Nan, T. *et al.*	$SrIrO_3$/Py	20 nm	—	0.58	300 K
2019[4]	Liu, L. *et al.*	$SrRuO_3$/$SrIrO_3$	8 nm	—	0.86	70 K
2019[5]	Everhardt, A. S. *et al.*	$SrIrO_3$/Py	13 nm	—	0.33	300 K
2019[6]	Wang, H. *et al.*	$SrIrO_3$/$Co_{1-x}Tb_x$	30 nm	—	1.1	300 K
2019[7]	Ou, Y. *et al.*	$SrRuO_3$/Co	10 nm	—	0.1 (300 K) 0.23 (60 K)	60-300 K
2016[8]	Wahler, M. *et al.*	$SrRuO_3$/$La_{0.7}Sr_{0.3}MnO_3$	1.2 nm	—	0.027	190 K
2021[9]	Wei, J. *et al.*	$SrRuO_3$/Py	6 nm	—	0.04-0.89	300 K
2021[10]	Zhou, J. *et al.*	$SrRuO_3$/Py	20 nm	—	0.015-0.15	300 K
2020[11]	Bose, A. *et al.*	IrO_2/Ir/Py	5 nm	—	0.65 (30 K) 0.08 (300 K)	30-300 K
2020[12]	Ueda, K. *et al.*	IrO_2/Py	7 nm	—	0.09	300 K

The comparison of the effective magnetic field and SOT efficiency of 4*d*/5*d* transition metal oxides are added in Section 10 of Supplementary Information, and the corresponding discussion is added in the revised manuscript (Page 6, Line 238-242).

Comment 2: *"In Fig. 4b, isn't Hex related to the switching current?"*

Reply: The switching current is indeed related to the H_{ex}. In order to confirm this regulation, we carry out a series of switching measurements, in which H_{ex} is increased from 0 Oe to -500 Oe as shown in Fig. R12.

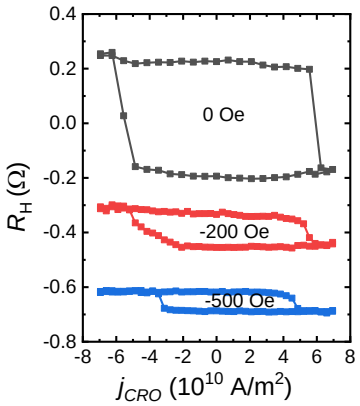

Fig. R12 Current-induced magnetization switching of Hall bars device when different in-plane magnetic fields (from 0 Oe to -500 Oe) are applied along the direction of the current. The loops are shifted for better visualization.

We can see that the switching current decreases obviously with this large field range. At the same time, R_H decreases correspondingly, which can be attributed to the decrease of the out-of-plane magnetic moment under the application of in-plane magnetic field. However, due to the small increment of magnetic field between -20 and 40 Oe in the manuscript, the change of critical switching current is not obvious.

Comment 3: *"In Fig. 4c and d, the grey colors correspond to +Mz and –Mz, respectively. I am wondering why the grey color does not represent the same direction. Additionally, for example, in Fig. 4c, I intuitively assume that the grey color may correspond to the in-plane direction of magnetization. If the magnetization is along the in-plane direction, which color is presented in the image?"*

Reply: We are sorry for not illustrating the method of MOKE measurement. This measurement is based on background-subtracted MOKE. To enhance the contrast, the background in the whole image was subtracted, and the whole image in the initial state maintains the same color (grey) though the pillar area is in magnetic polarity state. In Figs. 4c and 4d, we initialize the magnetization to the $+M_z$ state and $-M_z$ state, respectively, and the images of initial state are both grey after the background is subtracted. Thus, the grey color does not represent the same direction. When the magnetic polarity state changes, the color in pillar area changes accordingly, while the color outside the pillar area remains unchanged. Although the grey color does not represent the same magnetic polarity state, the $-M_z$ state is always brighter than the $+M_z$ state. This MOKE measurement method is widely used to characterize magnetic polarity [Liu, L. *et al.* Nat. Nanotechnol. 16, 277-282 (2021); Davies, C.S. *et al.* Nature, 628, 540–544 (2024)].

The relative caption is added in the revised manuscript (Page 17, Line 576-578).

Same as the case of perpendicular magnetization, when the magnetization is along the in-plane direction, the magnetic polarity state is initialized to the grey color and the switching between the magnetic polarity state $+M_y$ and $-M_y$ is represented by contrast. For example, when the $-M_y$ state is represented by grey color, the magnetization is switched to $+M_y$ state and represented by dark color [Wang, Y. *et al.* Nat. Commun. 8, 1364 (2017); Shi, S. *et al.* Nat. Nanotechnol. 14, 945–949 (2019)].

Comment 4: *"The curves are shifted for visualization in Fig. 4b. Including information about the baseline resistance in the caption would be helpful for readers."*

Reply: We thank the reviewer for this suggestion. The baseline resistance of the loops is about 1.6 Ω, which is generated by misalignment of contacts. To help with reading, the information about the baseline resistance is added in the caption in the revised manuscript (Page 17, Line 575).

Comment 5: *"In the switching experiment shown in Fig. 4, the current is divided into two paths: the CRO channel and metallic multilayers. The portion of the current for each of the two paths should be clarified in the manuscript."*

Reply: We thank the reviewer for the suggestion. Here we clarify the portion of the current in different materials. For the Ta (2 nm)/MgO (2 nm)/CoFeB ($Co_{20}Fe_{60}B_{20}$, 1.2 nm)/Ti (3 nm)/CRO (9 nm) device shown in Fig. 4, the critical current is 9 mA. The resistivities of CRO (9 nm) and the

PMA structure CoFeB (1.2 nm)/Ti (3 nm) layers (the Ta layer will be oxidized in air), can be obtained from standard four-probe measurements. We get the resistivity for each layer ρ_{CRO} = 1.1×10^{-5} Ω·m and $\rho_{PMA} = 4.7\times10^{-6}$ Ω·m. The width of CRO layers is 16 μm and the PMA layers are etched into round pillar with a diameter of 10 μm.

The resistivity of round pillar PMA layers can be calculated as:

$$R_{PMA} = \int_{-r}^{r} \frac{\rho_{PMA} dl}{s} = \frac{\pi \rho_{PMA}}{2t_{PMA}}$$

The critical current density by considering the parallel circuit model can be estimated as:

$$I_{CRO} = I_{all} \frac{R_{PMA}}{R_{CRO} + R_{PMA}}$$

$$= I_{all} \frac{\frac{\pi \rho_{PMA}}{2t_{PMA}}}{\frac{\rho_{CRO} l_{CRO}}{w_{CRO} \times t_{CRO}} + \frac{\pi \rho_{PMA}}{2t_{PMA}}}$$

$$= 9\ mA \times \frac{\frac{\pi \times 4.7 \times 10^{-6}\ \Omega \cdot \mathrm{m}}{2 \times 4.2\ nm}}{\frac{1.1 \times 10^{-5}\ \Omega \cdot \mathrm{m} \times 10\mu\mathrm{m}}{16\ um \times 9\ nm} + \frac{\pi \times 4.7 \times 10^{-6}\ \Omega \cdot \mathrm{m}}{2 \times 4.2\ nm}}$$

$$= 6.3\ mA$$

$$J_{CRO} = I_{CRO} \times \frac{1}{w_{CRO} \times t_{CRO}} = 6.3\ mA \times \frac{1}{16\ um \times 9\ nm} = 4.4 \times 10^{10}\ \mathrm{Am}^{-2}$$

Therefore, thirty percent portion of the current flows into the PMA structure, the contribution of current induced torque from the Ti layer is negligible due to the extremely small spin Hall angle of Ti [Du, C. *et al.* Phys. Rev. B 90, 140407 (2014)]. The critical current density for the field-free switching is as low as 4.4×10^{10}Am^{-2}, when considering the shunt effect.

The shunting effect is clarified in the revised manuscript (Page 9, Line 334-336) and the corresponding calculation is added in Section 17 of Supplementary Information.

Comment 6: *"On page 6, the authors explain that 'The influence of the Py/CRO interface is very limited...' This sentence may mislead readers because the authors describe an out-of-plane polarized spin current resulting from the relaxation of oxygen octahedral tilt/rotation near the interface."*

Reply: We agree that this sentence "The influence of Py/CRO interface is very limited and CRO layers still maintains high symmetry without lattice distortion" may mislead readers, thus, this sentence is replaced by "The oxygen octahedral tilt/rotation keeps uniform in CRO layers near the Py/CRO interface, and CRO layers still maintains high symmetry." in the revised manuscript (Page 7, Line 261-262).

Comment 7: *"The experiment on the switching of perpendicular magnetization involves x- and y-direction polarized current, as well as z-direction polarized current. What are the relative values of these three terms?"*

Reply: The *x*-, *y*- and *z*-direction polarized spin current generated from CRO is analyzed by ST-FMR measurement. The efficiencies of *z*-direction torque are determined to be 0.0086, which is comparable to that generated from WTe_2 [MacNeill, D. *et al. Nat. Phys.* 13, 300-305 (2017)] and $MnPd_3$ [DC, M. *et al. Nat. Mater.* 22, 591–598 (2023)]. The *z*-direction polarized spin current

provides in-plane effective field for field-free switching. Since the x-direction damping-like torque is forbidden by crystal symmetry and can be ignored, we mainly focus on the y- and z-direction damping-like torque. The relative values of z- and y-direction torque, i.e. $\theta_z^{DL}/\theta_y^{DL}$ is about 0.0062. The spin-polarization canting angle in CRO films is sufficient for field-free deterministic switching of perpendicular magnetization [Lee, DK. *et al.* Sci. Rep. 10, 1772 (2020)].

Comment 8: *"The authors claimed that a very low current density is required for switching. A comparison with other field-free systems is recommended."*

Reply: We thank the reviewer for the comment. We summarize the critical current density for field-free switching in different heterostructures as shown in Table 1. We can see that CoFeB/CRO system requires lower current density than most of heterostructures. Although the critical current density in $SrRuO_3/SrIrO_3$ heterostructure is smaller than that in CoFeB/CRO heterostructure, the working temperature of $SrRuO_3/SrIrO_3$ heterostructure is below room temperature. The comparison with other field-free systems indicates the high efficiency of field-free switching perpendicular magnetization in CoFeB/CRO system.

The corresponding discussion is added in the revised manuscript (Page 8, Line 332-334) and the summary of critical current density in different heterostructures is added in Section 16 of Supplementary Information.

Table 1. Summary of critical current density for field-free switching in different heterostructures.

Year	Author	Heterostructures	Critical current density ($\times 10^{10}$Am^{-2})	Temperature
this work	Han, F. *et al.*	$CaRuO_3$/CoFeB	6.3	300 K
2019[2]	Liu, L. *et al.*	$SrRuO_3/SrIrO_3$	4.6	70 K
2022[13]	Kao, IH. *et al.*	$WTe_2/Fe_{2.78}GeTe_2$	9.8	190 K
2023[14]	Liu, Y. *et al.*	$TaIrTe_4$/CoFeB	7.6	300 K
2021[15]	You, Y. *et al.*	$Mn_3SnN/(Co/Pd)_3$	9	300 K
2023[16]	DC, M. *et al.*	$MnPd_3$/Co	11	300 K
2021[17]	Chen, X. *et al.*	$Mn_2Au/(Co/Pd)_3$	55	300 K
2022[18]	Karube, S. *et al.*	RuO_2/Co	30	300 K
2021[19]	Zheng, Z. *et al.*	$Co_{1-a}Tb_a$	9	300 K
2016[20]	Oh, YW. *et al.*	IrMn/CoFeB	42	300 K
2016[21]	Lau, YC. *et al.*	Pt/CoFe/Ru /CoFe/IrMn	20	300 K

Comment 9: *"Please discuss the dot size effect and pulse width effect on critical switching current density."*

Reply: We thank the reviewer for the suggestion. In order to clarify the dot size effect, we fabricate a series of samples, in which the PMA layers are etched into dots with diameters of 10 μm, 5μm and 3μm, respectively. As the dot size reduces, the R_H value decreases accordingly. The perpendicular

magnetization can be switched by applying pulsed current as shown in Fig. R13a. In order to compare the critical current density in devices with different dot sizes, the current in PMA layers is extracted. The perpendicular magnetization is switched nearly at the same current density, so the size of the dot has little effect on the density of critical switching current.

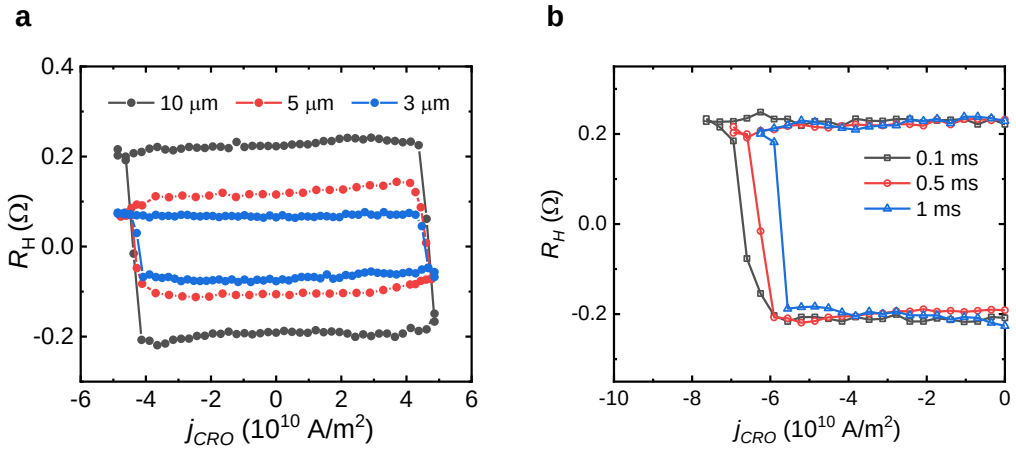

Fig. R13 a, Current-induced magnetization switching of the dot with different size. b, Current-induced magnetization switching when pulsed current with different width is applied.

In order to analyze the pulse width effect on critical switching current density, we measure the magnetization switching curves with different pulse widths as shown in Fig. R13b. When the pulse width increases from 0.1 mA to 1 mA, the critical switching current density decreases, which can be attributed to the increase of temperature due to the Joule heating. This behavior is consistent with theoretical analysis [Diao, Z. *et al.* J. Phys., Condens. Matter, 19, 165209, (2007); Huai, Y. AAPPS Bulletin December, 18, 6, (2008)].

Comment 10: *"Please describe the role of Ti between CRO and CoFeB."*

Reply: The Ti layer was introduced to get perpendicularly magnetized CoFeB layers, and the SOT contribution from the Ti layer is negligible due to the extremely small spin Hall angle of Ti [Du, C. *et al.* Phys. Rev. B 90, 140407 (2014)]. Ti as a buffer layer is widely used to stabilize the perpendicular magnetization of CoFeB layers [Liu, Y. *et al.* Nat. Electron. 6, 732–738 (2023); Cao, C. *et al. Nat. Commun.* 14, 5873 (2023)].

The role of Ti layer is added in the revised manuscript (Page 8, Line 316-318).

Minor comments

- In Fig. 3a, the arrowhead of the spin current (J_S) may be obscured by other objects.

- In Fig. 4a, inserting the direction of Hex is helpful for readers to easily understand the experimental set-up.

- In addition to current density, information about the actual current itself in Fig. 4b may be helpful for future experiments conducted by others.

- The insertion of a scale bar or a description of dot size in the caption of Fig. 4c and d is recommended.

Reply: We thank the reviewer for these valuable suggestions. The arrowhead of the spin current in

Fig. 3a is updated in the revised manuscript and also shown in Fig. R14a.
The direction of H_{ex} in Fig. 4a is added in the revised manuscript and also shown in Fig. R14b.
The information about the actual current is added in the revised manuscript (Page 9, Line 330).
The scale bars in Figs. 4c and 4d are added as shown in Fig. R14c and the description of dot size in the caption is added in the revised manuscript (Page 17, Line 573).

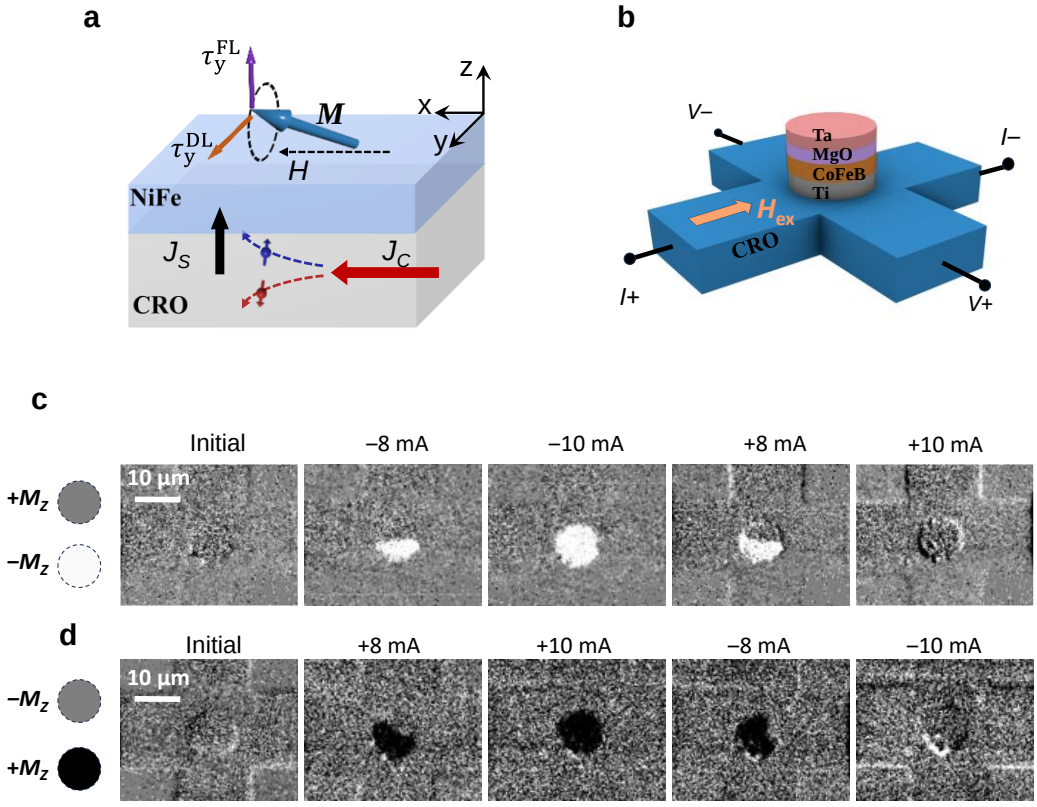

Fig. R14 a, Schematic of ST-FMR measurement in Fig. 3a of the manuscript. b, Schematic of the Ta/MgO/CoFeB/Ti/CRO Hall bar device for switching measurements in Fig. 4a of the manuscript. c, MOKE images of the field-free SOT induced magnetization switching in Fig. 4c of the manuscript.

References

1. Li, S. *et al.* Room temperature spin-orbit torque efficiency and magnetization switching in $SrRuO_3$-based heterostructures. *Phys. Rev. Mater.* **7**, 024418 (2023).
2. Li, P. *et al.* Large Spin-Orbit-Torque Efficiency and Room-Temperature Magnetization Switching in $SrIrO_3$/Co-Fe-B Heterostructures. *Phys. Rev. Appl.* 19, 024076 (2023).
3. Nan, T. *et al.* Anisotropic spin-orbit torque generation in epitaxial $SrIrO_3$ by symmetry design. *Proc. Natl. Acad. Sci. U.S.A.* **116**, 16186-16191 (2019).
4. Liu, L. *et al.* Current-induced magnetization switching in all-oxide heterostructures. *Nat. Nanotechnol.***14**, 939-944 (2019).
5. Everhardt, A. S. *et al.* Tunable charge to spin conversion in strontium iridate thin films. *Phys. Rev. Mater.* **3**, 051201 (2019).

6. Wang, H. *et al.* Large spin-orbit torque observed in epitaxial $SrIrO_3$ thin films. *Appl. Phys. Lett.* **114**, 232406 (2019).
7. Ou, Y. *et al.* Exceptionally High, Strongly Temperature Dependent, Spin Hall Conductivity of $SrRuO_3$. *Nano Lett.* **19**, 3663–3670 (2019).
8. Wahler, M. *et al.* Inverse spin Hall effect in a complex ferromagnetic oxide heterostructure. *Sci. Rep.* **6**, 28727 (2016).
9. Wei, J. *et al.* Enhancement of Spin-Orbit Torque by Strain Engineering in $SrRuO_3$ Films. *Adv. Funct. Mater.* 31, 21000 (2021).
10. Zhou, J. *et al.* Modulation of Spin-Orbit Torque from $SrRuO_3$ by Epitaxial-Strain-Induced Octahedral Rotation. *Adv. Mater.* 33, 2007114 (2021).
11. Bose, A. *et al.* Effects of Anisotropic Strain on Spin–Orbit Torque Produced by the Dirac Nodal Line Semimetal IrO_2. *ACS Appl. Mater. Interfaces* 12, 55411–55416 (2020).
12. Ueda, K. *et al.* Spin-orbit torque generation in NiFe/IrO_2 bilayers. Phys. Rev. B 102(13), 134432 (2020).
13. Kao, IH. *et al.* Deterministic switching of a perpendicularly polarized magnet using unconventional spin-orbit torques in WTe_2. *Nat. Mater.* **21**, 1029–1034 (2022).
14. Liu, Y. *et al.* Field-free switching of perpendicular magnetization at room temperature using out-of-plane spins from $TaIrTe_4$. *Nat. Electron.* **6**, 732–738 (2023).
15. You, Y. *et al.* Cluster magnetic octupole induced out-of-plane spin polarization in antiperovskite antiferromagnet. *Nat. Commun.* **12**, 6524 (2021).
16. DC, M. *et al.* Observation of anti-damping spin-orbit torques generated by in-plane and out-of-plane spin polarizations in $MnPd_3$. *Nat. Mater.* **22**, 591–598 (2023).
17. Chen, X. *et al.* Observation of the antiferromagnetic spin Hall effect. *Nat. Mater.* **20**, 800–804 (2021).
18. Karube, S. *et al.* Observation of Spin-Splitter Torque in Collinear Antiferromagnetic RuO_2. *Phys. Rev. Lett.* **129**, 137201(2022).
19. Zheng, Z. *et al.* Field-free spin-orbit torque-induced switching of perpendicular magnetization in a ferrimagnetic layer with a vertical composition gradient. *Nat. Commun.* **12**, 4555 (2021).
20. Oh, YW. *et al.* Field-free switching of perpendicular magnetization through spin-orbit torque in antiferromagnet/ferromagnet/oxide structures. *Nat. Nanotech.* **11**, 878–884 (2016).
21. Lau, YC. *et al.* Spin-orbit torque switching without an external field using interlayer exchange coupling. *Nat. Nanotech.* **11**, 758–762 (2016).

REVIEWER COMMENTS

Reviewer #2 (Remarks to the Author):

There were a lot of speculation about the physical properties, but most of the corrections are significant. I guess that the additional experiments on Reviewer 2 require great deal of efforts. I thank to the authors for the attentive replies. Finally, I request a reconsideration of the comparison with the Fermi surfaces reported in ARPES.

In fig. R8 (right below [Liu, Y. et al. Phys. Rev. B, 98, 041110 (2018).]), you can see few FS in the 1st BZ. This is due to a property of ARPES. Maybe, Liu et al. are inadequately described. Precisely, we have to look at ‘the FS in the 2nd BZ’. Here we see the two most characteristic cylindrical Fermi surfaces in the CRO. They are open only in the kz direction, giving a strong anisotropy to conduction. In such a highly anisotropic system, the current flows depend on the crystal orientation. The electronic structure must be compared to the band calculation and discussed in relation to the orientation of the measured current.

If the requested comparison with ARPES is reconsidered well, we believe it deserves to be published for 'Nature communications'. If the correction is achieved without problems, no further review by me would be necessary.

Reviewer #3 (Remarks to the Author):

The issues I commented on are clearly addressed, so I recommend this manuscript for publication.

Response Letter

Reply to Reviewer #2

Comment: *There were a lot of speculation about the physical properties, but most of the corrections are significant. I guess that the additional experiments on Reviewer 2 require great deal of efforts. I thank to the authors for the attentive replies. Finally, I request a reconsideration of the comparison with the Fermi surfaces reported in ARPES.*

In fig. R8 (right below [Liu, Y. et al. Phys. Rev. B, 98, 041110 (2018).]), you can see few FS in the 1st BZ. This is due to a property of ARPES. Maybe, Liu et al. are inadequately described. Precisely, we have to look at 'the FS in the 2nd BZ'. Here we see the two most characteristic cylindrical Fermi surfaces in the CRO. They are open only in the kz direction, giving a strong anisotropy to conduction. In such a highly anisotropic system, the current flows depend on the crystal orientation. The electronic structure must be compared to the band calculation and discussed in relation to the orientation of the measured current.

If the requested comparison with ARPES is reconsidered well, we believe it deserves to be published for 'Nature communications'. If the correction is achieved without problems, no further review by me would be necessary.

Reply: We thank the reviewer for the recognition of our efforts and the recommendation of this manuscript for publication in *Nature Communications* after minor revision. The suggestions greatly help us to improve our manuscript. We agree that the electronic structure of CRO is anisotropic, in agreement with the observation of the ARPES experiments. And it contributes to the anisotropy of the spin Hall effect.

To begin with, we review the anisotropic electronic structure of CRO. The surface states spectra of orthorhombic CRO at Fermi energy for the (001) and the (100) surfaces are obtained from DFT calculations, as shown in Figs. R1 **a-b**. The surface states of the (001) and the (100) surfaces show distinct features, and indicate that Fermi surfaces are open only in the k_z direction. The surface spectra from DFT calculations qualitatively match the experimental results of ARPES [Liu, Y. et al. Phys. Rev. B, 98, 041110 (2018)].

The deep relation between the anisotropy of band structure and the spin Hall effect can be described by the theoretical formula of the spin Hall effect

$$\sigma_{\alpha\beta;\gamma}(\omega) = -\frac{e^2}{\hbar}\int_{BZ}\frac{d^3k}{(2\pi)^3}\Omega_{\alpha\beta;\gamma}(k), \tag{R1}$$

$$\Omega_{\alpha\beta;\gamma}(k) = -2\hbar^2\sum_n f_{nk}\sum_{n'\neq n}\mathrm{Im}\left[\frac{\langle nk|j_{\alpha;\gamma}|n'k\rangle\langle n'k|v_\beta|nk\rangle}{\left(E_{n'}-E_n\right)^2-(\hbar\omega+i\delta)^2}\right], \tag{R2}$$

where the spin current operator is defined as $j_{\alpha;\gamma} = \frac{1}{2}\{s_\gamma, v_\alpha\}$. s_γ is the spin operator and it is independent of the band structures. v_α, v_β is the velocity operator and it can be associated with the band structures through

$$\langle v_\alpha\rangle = \frac{1}{\hbar}\left\langle\psi\left|\frac{\partial H}{\partial k_\alpha}\right|\psi\right\rangle = \frac{1}{\hbar}\frac{\partial\varepsilon}{\partial k_\alpha}. \tag{R3}$$

Since the Fermi surface is the slice of the band structures at a fixed energy level, its anisotropic shape reflects the anisotropy of the band dispersion, i.e., the $\frac{\partial \varepsilon}{\partial k_\alpha}$. Besides, the energy differences $(E_{n'} - E_n)^2$ in the denominator are also determined by the band structures.

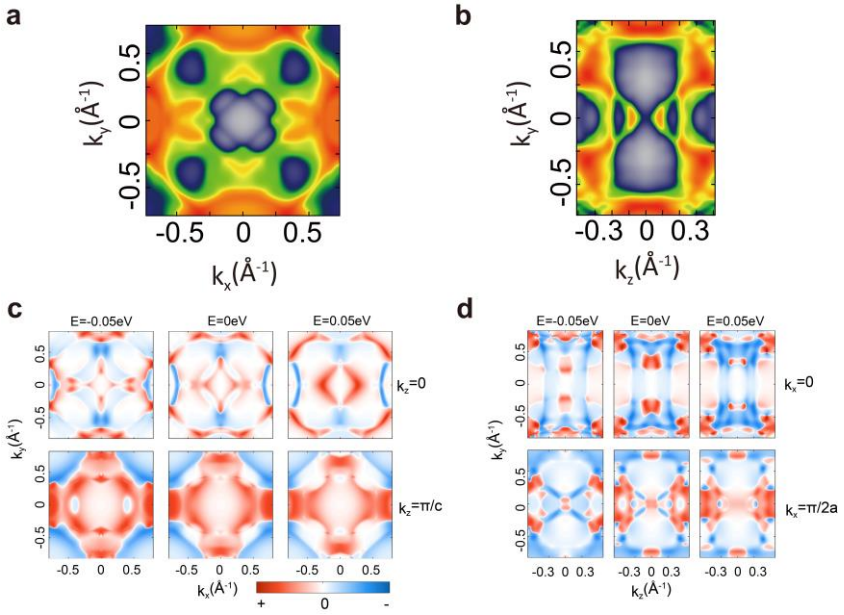

Fig. R1 **a, b** Surface states of orthorhombic CRO at Fermi energy for the (001) (**a**) and the (100) (**b**)surfaces, respectively. **c, d** Distributions of the spin Berry curvature $\Omega_{zx;y}$ at different energy levels (left panel: E = -0.05 eV, middle panel: E = 0 eV, right panel: E = 0.05 eV), for k_z cuts (**c**) and k_x cuts (**d**).

Following the reviewer's suggestion, we show the effect of anisotropic electronic structure on the spin Hall conductivity (SHC) from two aspects. Firstly, we calculate the *k*-resolved distributions of the spin Berry curvature and find a correspondence with the band anisotropy. We plot the distribution of $\Omega_{zx;y}$ as an example in Figs. R1 **c-d**. It can be seen from the spin-Berry-curvature distributions for the (001) film, that the pattern and the strength along the k_x and k_y directions are very close for different *k*-planes and energy levels. But for the (100) film, the pattern and the strength along k_y and k_z directions show obvious differences. The calculated spin-Berry-curvature distributions are consistent with the anisotropic electronic structure as shown in Figs. R1 **a-b**.

Secondly, we calculate the anisotropy of the SHC in relation to the orientation of the measured current. We compare the SHC component $\sigma_{zx;y}$, which has been discussed in the manuscript, with $\sigma_{xy;z}$ (the induce of SHC corresponding sequentially to the response current, the applied electric field, and the spin polarization). The set-up planes of the applied and the response currents for the two terms are [010] and [001] planes, respectively. It can show the anisotropy between the z and y directions. From Fig. R2 we can see $\sigma_{zx;y}$ is about twice as much as $\sigma_{xy;z}$ at the Fermi energy (at E=0 eV). This difference owes to the directions of band dispersions involved in SHC in Eq. (R1), which includes v_z and v_x for $\sigma_{zx;y}$ and v_y and v_x for $\sigma_{xy;z}$. $\sigma_{zx;y}$ is enhanced by v_z due to the anisotropic fermi surface along z direction. Our calculations demonstrate that the magnitude of the response spin Hall current in CRO would rely on the measured current and the set-up plane.

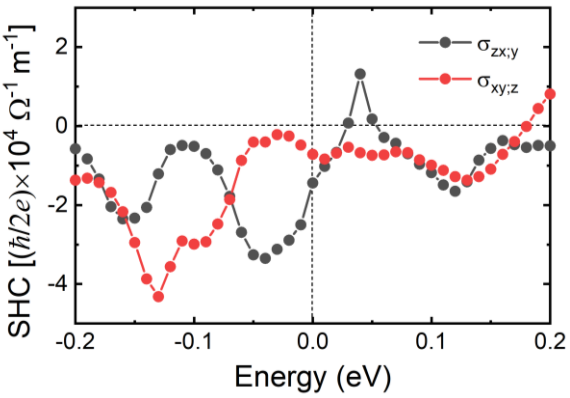

Fig. R2 $\sigma_{zx;y}$ and $\sigma_{xy;z}$ of the spin Hall conductivities in CRO, calculated from DFT results.

Consequently, we confirm that the spectra of Fermi surfaces calculated by DFT are anisotropic, which matches the ARPES results according to the comparison. This anisotropic electronic structure results in the anisotropy of spin Hall current that the magnitude depends on crystal orientation, which is consistent with the reviewer's inference.

In revision, the surface states spectra of orthorhombic CRO at Fermi energy, and the spin-Berry-curvature distributions are added in Section 6 of Supplementary Information, the corresponding discussion is added in the revised manuscript (Page 4, Line 160-163) and the reference [Liu, Y. et al. Phys. Rev. B, 98, 041110 (2018)] is cited.

Reply to Reviewer #3

Comment: *The issues I commented on are clearly addressed, so I recommend this manuscript for publication.*

Reply: We thank the reviewer for acknowledging our revision and for recommending its publication in *Nature Communications*.

REVIEWERS' COMMENTS

Reviewer #2 (Remarks to the Author):

The issue that I commented on has been addressed.
I recommend the manuscript for publication of Nature communications.

Reply to Reviewer #2

Comment: *The issue that I commented on has been addressed.*
I recommend the manuscript for publication of Nature communications.

Reply: We thank the reviewer for taking efforts to review and recommendation of this manuscript for publication in *Nature Communications*.